Indirect tension test of epoxy asphalt mixture using microstructural finite-element model

Wang Jiangyang   Qian Zhendong

(Intelligent Transportation System Research Center, Southeast University, Nanjing 210096, China)

Abstract: A finite-element model of the thermosetting epoxy asphalt mixture (EAM) microstructure is developed to simulate the indirect tension test (IDT). Image techniques are used to capture the EAM microstructure which is divided into two phases: aggregates and mastic. A viscoelastic constitutive relationship, which is obtained from the results of a creep test, is used to represent the mastic phase at intermittent temperatures. Model simulation results of the stiffness modulus in IDT compare favorably with experimental data. Different loading directions and velocities are employed in order to account for their influence on the modulus and the localized stress of the microstructure model. It is pointed out that the modulus is not consistent when the loading direction changes since the heterogeneous distribution of the mixture internal structure, and the loading velocity affects the localized stress as a result of the viscoelasticity of the mastic. The study results can provide a theoretical basis for the finite-element method, which can be extended to the numerical simulations of asphalt mixture micromechanical behavior.

Key words: microstructure; epoxy asphalt mixture; image techniques; finite-element model; indirect tension test

doi: 10. 3969/j. issn. 1003 – 7985. 2011. 01. 014

Asphalt mixtures can be described as a multiphase material containing aggregates, mastic cement (including asphalt binder and fine particles) and air voids. The volumetric properties of the three compositions and the viscoelasticity of the asphalt cause the complexity of the asphalt mixture's mechanical behavior. However, studying the complex constitutive behavior of asphalt mixtures requires capturing their microstructure and modeling the stress-strain behavior of the binder.

Recently, many researchers have investigated the micromechanical behavior of asphalt mixtures using numerical simulations combined with image techniques. Two numerical methods have been utilized to simulate the micromechanical behavior of asphalt mixtures, namely the finite-element method (FEM) and the discrete-element method (DEM). These two methods have their respective pros and cons[1], and in this paper the former is used. Bahia et al. [2] conducted finite element analyses using an idealized internal structure of asphalt mixtures. Kose et al. [3] utilized image tech-

niques and finite-element analysis to analyze the strain distribution within asphalt mixtures. Yu et al. [4] used X-ray computed tomography images to build a microstructure of asphalt mixtures for the IDT test and analyzed the effects of air voids distributions. The above researchers all assumed in their studies that linear elastic properties were included for the binder and the aggregate, which did not agree with the fact that the mastic is viscoelastic. Therefore, Abbas et al. [5] incorporated a nonlinear viscoelastic material model in the FEM to analyze the asphalt mixture microstructure. The model geometry was described using the same procedure presented by Papagiannakis et al[6]. The viscoelastic behavior of the asphalt mastic was defined using a nonlinear viscoelasitc material model, which was numerically solved using a convolution integral approach. To account for the asphalt binder nonlinearity, the mechanical parameters were updated during the analysis according to the strain level within each element. Two-dimensional four-node bilinear elements were used in these FEM-based studies.

The thermosetting epoxy asphalt mixture (EAM), which is of high strength, high resistance to permanent deformation, low temperature cracking, etc. [7], usually performs differently from the normal thermoplastic material such as the hot mix asphalt (HMA). However, the above-mentioned researches were often conducted on thermoplastic materials, and few researches on the micromechanical behavior of thermosetting materials have been retrieved.

In order to investigate the micromechanical behavior of the EAM, this paper uses creep tests and image techniques to build a microstructure finite-element model. On the basis of this model, the IDT numerical simulation is used to study the stress and strain distribution of the internal structure and to analyze the influence of the loading direction and velocity on the IDT.

1 Microstructural Finite-Element Model

1.1 Material properties

The aggregate material is normally much stiffer than the mastic, and thus aggregates are taken as rigid particles. On the other hand, the asphalt mastic is a compliant material with viscoelasitc behavior, especially at intermediate and high temperatures[8]. Therefore, laboratory experimental data are needed to determine the material properties used in the finite-element model.

In this paper, the creep test at 15 ℃ is used to measure the viscoelastic properties of the epoxy asphalt mastic. The binder used in the test is 2910-type domestic epoxy asphalt, which is composed of two components marked as A and B. Component A is the epoxy resin while component B consists of petroleum asphalt and a curing agent. With reference to

the gradation of the Second Nanjing Yangtze River Bridge (The normal maximum aggregate size is 13. 2 mm.)[9], asphalt mastic is prepared by mixing diabase aggregate particles (smaller than 2. 36 mm) and limestone powder with asphalt binder, and the mastic gradation is given in Tab. 1. The asphalt content of the mastic, which is calculated by specific surface area[10], is 11. 02%.

Tab. 1   Gradation of the EA mastic

Sieve size/mm	2. 36	1. 18	0. 60	0. 30	0. 15	0. 075
Passing rate of different sieves/%	100	78. 3	56. 7	44. 2	30. 8	17. 5

The response of the Burgers model due to the application of the creep load (constant stress 0. 1 MPa) is characterized using the creep compliance, $J(t)$, which is equal to the resulting strain function divided by the applied stress. The test data are fitted by the creep equation:

$$J(t) = \frac{1}{E_1} + \frac{t}{\eta_1} + \frac{1}{E_2}\left(1 - \exp\left(-\frac{E_2}{\eta_2}t\right)\right) \qquad (1)$$

where E_1 and E_2 are the Maxwell and Kelvin spring stiffnesses, respectively; η_1 and η_2 are the Maxwell and Kelvin dashpot damping coefficients, respectively.

The E_1, E_2, η_1, η_1 are $1. 92 \times 10^7$, $1. 17 \times 10^7$, $2. 91 \times 10^{11}$, $1. 91 \times 10^9$ fitted to the test data, respectively, which presents similar elasticity but lower viscosity than other thermoplastic asphalt mastic[10]. The master curve is shown in Fig. 1.
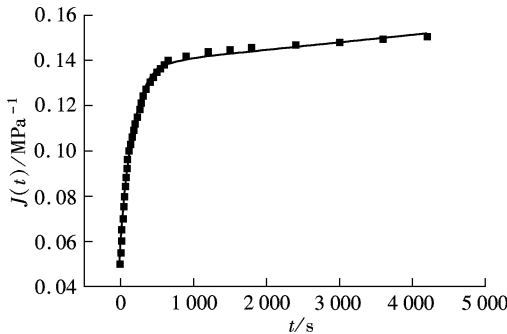

Fig. 1   Creep compliance $J(t)$ of the Burger model vs. time

The mechanical behavior of viscoelastic material can be presented by the Prony series of relaxation moduli in the finite element software[10]. In this paper, the four parameters of the Burgers model are converted into the Prony series using Matlab software, which are given below: $g_1 = 0. 623\ 3$; $g_2 = 0. 376\ 7$; $\tau_1 = 166. 470\ 7$ s; $\tau_2 = 1. 08 \times 10^5$ s.

1. 2   Image processing

In order to capture the real EAM microstructure, simulation material models are generated by analyzing the photographic data of actual asphalt samples. The standard super pave mix procedure is employed to prepare the samples, and 6. 8% is determined as the optimum asphalt content based on the Marshall mixture design procedure. After curing of EAM for 5 h at 130 ℃, the standard 102-mm-diameter indirect tension specimen is cut for image processing.

A digital camera provides an electronic RGB image of the sectioned specimen, and this image is converted to grayscale using ImagePro software as shown in Fig. 2 (a). Each

grayscale pixel has a brightness value ranging from 0 (black) to 255 (white). A grayscale threshold is applied to convert the original image to a binary (black and white) file and the image is shown in Fig. 2(b). The white color represents aggregates greater than 2. 36 mm, while black represents the phase combining the epoxy asphalt binder and fine aggregates smaller than 2. 36 mm, which is referred to as the mastic. In this paper, the air voids are assumed not involved since the porosity of the sample is 2. 6%, less than other normal asphalt mixtures. This file is the input used to develop the finite element mesh and assign material properties.
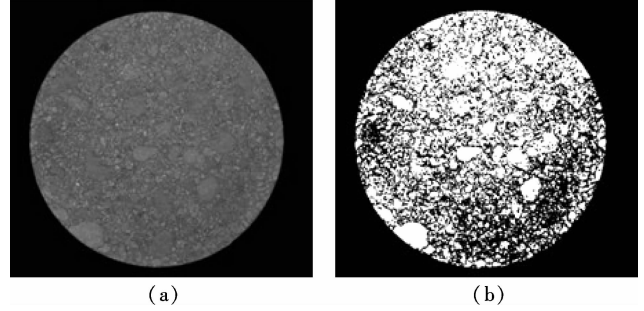

Fig. 2   Image processing for indirect tension sample. (a) Grayscale image; (b) Binary image with segmentation technique

1. 3   Model building

By DXF interface of AutoCAD 2004, the above file is introduced into the finite element software to model the EAM microstructure.

Before analysis, the contact behavior between aggregates and mastic is assumed completely continuous. Quadrilateral-dominated elements are used to differentiate elements relative to aggregates and those relative to the mastic, and the seed density of the former is 1. 0, the latter is 0. 6. Free mesh generation is obtained by the mesh division algorithm and it is shown in Fig. 3.
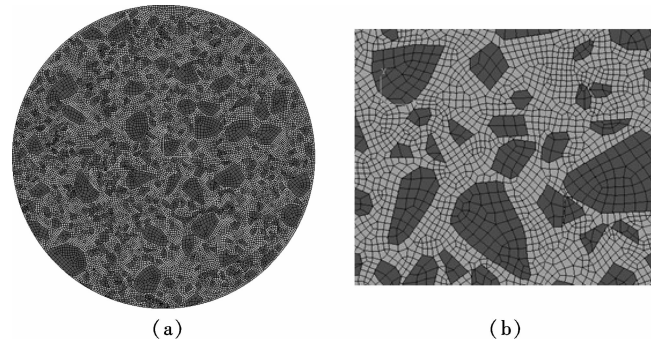

Fig. 3   Mesh generation of EAM microstructure. (a) Mesh generation; (b) Meshing style and seed density

When at 15 ℃, the diabase aggregate phase of the microstructure is modeled using linear elastic properties with an elastic modulus of 30 GPa assumed and a Poisson's ratio of 0. 3[8]. On the other hand, the second phase which is the mastic in the model is defined as viscoelastic properties that can be presented by the Prony series of relaxation moduli as previously obtained in section 1. 1. When at −15 ℃, Abbas[8] reported that the stiffness of the asphalt binder significantly increased at low temperatures and exhibited signs of

less time-dependency, whereby small strain accumulations were noticed as compared with that at high temperatures. Therefore, an elastic modulus of 35 GPa is assumed for the aggregate and an elastic modulus of 700 MPa is assumed for the epoxy asphalt mastic, which can be measured in a bending beam rheometer (BBR) test. The Poisson's ratio is 0.3 and 0.35 for the aggregate and the mastic, respectively.

According to standard test methods[11], a controlled-strain vertical loading on the top of the specimen is applied; the width of splitting strip is 12.7 mm, and a unified displacement rate of 50 mm/min is performed for convenient comparative analysis. The displacement of the bottom nodes, whose width zone is 12.7 mm, is restricted in the horizontal and vertical directions. The loading and boundary conditions are illustrated in Fig. 4.
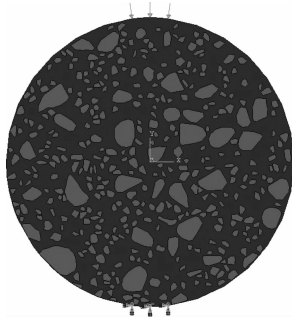

Fig. 4 Loading and boundary condition

2 Finite-Element Simulation of IDT and Discussion

2.1 Verification of stiffness modulus

Since the asphalt mixture is a heterogeneous composite material consisting of aggregates, asphalt mastic and air voids, the localized stress and strain vary significantly along the loading axle as a result of respective material properties when using finite-element software to model the mechanical behavior of microstructures. The distributions of S_{xx} and ε_{xx} (including elastic and creep strain) at 15 ℃ and along the vertical axle are shown in Fig. 5, where the center of the sample is 0.
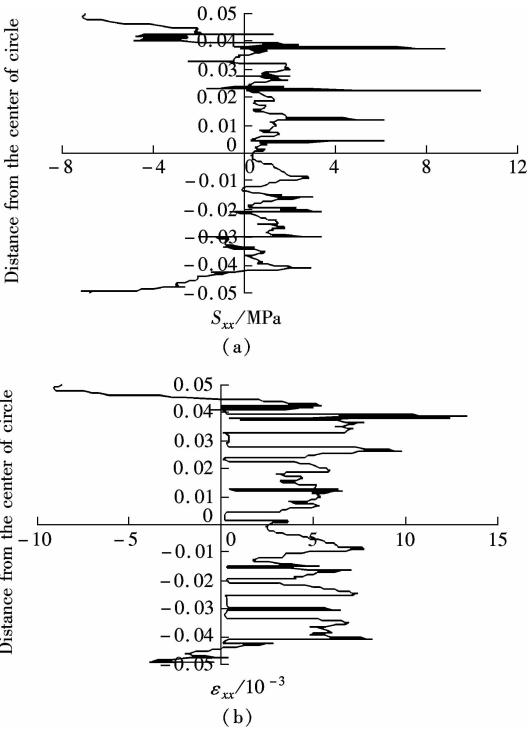

Fig. 5 S_{xx} and ε_{xx} distribution along the vertical axle. (a) S_{xx}; (b) ε_{xx}

The simulated stiffness modulus is calculated by averaging the stress and strain about 3/5 of the vertical central area in this paper, and compared with the modulus of the samples measured using IDT[12], which are given in Tab.2.

Tab. 2 Results comparison between numerical simulation and laboratory test   MPa

Index	Numerical simulation							Test results
	Step 1	Step 2	Step 4	Step 6	Step 8	Step 10	Average	
Stiffness modulus (15 ℃)	1 345	1 348	1 334	1 237	1 081	932	1 212.8	1 151.2
Stiffness modulus (−15 ℃)	4 307	4 102	4 662	4 460	3 961	3 640	4 188.7	3 887.5

The steps in Tab.2 are the incremental steps of the finite-element software, which are relevant to loading time. When the rate is 50 mm/min, each incremental step is 0.1 s.

It can be noticed that the numerical results at 15 ℃ have little deviation with those obtained from the laboratory test, which suggests sound material parameters for analyzing the time-dependent behavior of the Burger model. Furthermore, at low temperature (−15 ℃), moderate variations of the modulus during the increment steps are noticed, and there is an error of 7% between the average simulation results and the test. It can be illustrated that the asphalt mastic assumed as linear elastic properties at low temperature does not correspond with the fact. In general, the numerical simulation results match those in the test well and it is considered as a basis for further investigations. In addition, it is shown that the stiffness modulus at 15 ℃ and −15 ℃ of the EAM is 2 times and 3 times more than those of AC-16[10], respectively, as a result of the thermoplastic material.

2.2 Influence of loading direction

Because of the heterogeneousness of the asphalt mixtures, loading direction of IDT may affect the interaction of the internal structure. The stiffness moduli along four different loading directions, namely vertical, horizontal, inclined at 45° to left and to right, are used for numerical simulation, as shown in Fig.6 and the simulation results are given in Tab.3.
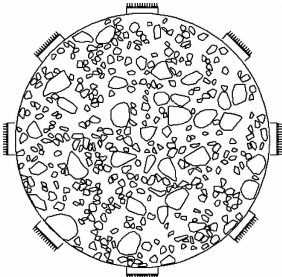

Fig. 6 Different loading directions

Tab. 3   Stiffness modulus in different loading direction (15 ℃)   MPa

Loading direction	Step 1	Step 2	Step 4	Step 6	Step 8	Step 10	Average
Vertical	1 345	1 348	1 334	1 237	1 081	932	1 212. 8
Horizontal	1 215	1 218	1 196	1 044	955	882	1 085. 0
Inclined to left	1 477	1 481	1 475	1 443	1 386	1 222	1 414. 0
Inclined to right	2 272	2 113	2 336	2 061	2 248	2 214	2 207. 3

It can be noticed that the stiffness modulus value is not consistent as the loading direction changes. It is mainly related to the heterogeneous and inhomogeneous distribution of the internal structure of the mixture. In stress paths, the size and amount of aggregates and the distribution of the mastic are not the same when loading in different directions. Therefore, these factors are assumed to have an influence on the distribution of the localized stress and strain.

The stiffness modulus in each direction presents some statistical characteristics. With regard to the asphalt mixture of definite gradation, there is some difference in its internal structure. But, on the basis of statistical law, the distributed feature of the aggregates has a good similarity in any of the directions when the mixture is uniform. Therefore, the modulus values of vertical, horizontal and inclined at 45° to the left have little difference.

In light of the above-mentioned, since the splitting stiffness modulus has both variability and statistical properties, it is suitable to use parallel tests, with several samples in order to obtain greater test effects.

2. 3   Influence of loading velocity

In this paper, − 15 ℃ and 15 ℃, 1 mm/min, 10 mm/min, 30 mm/min, 50 mm/min are selected as test temperature and loading velocities. The stress of the mixtures is numerically simulated using the microstructure finite-element method.

By computing, the relationships between loading velocity and splitting stiffness modulus are shown in Fig. 7.

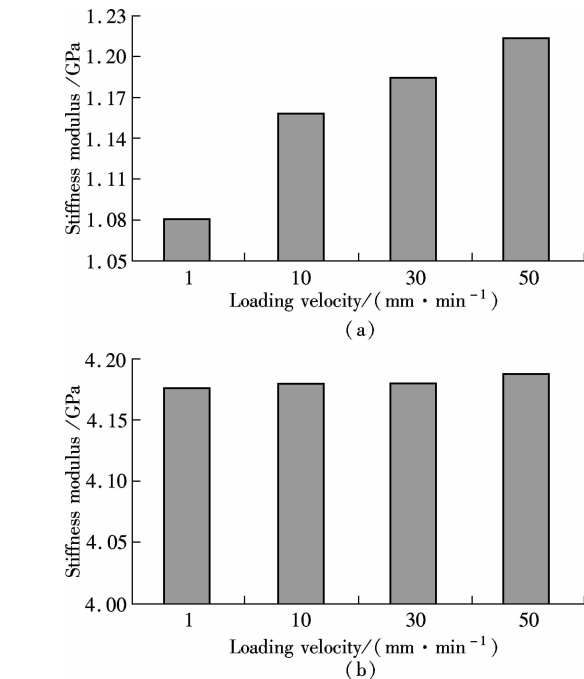From Fig. 7, it can be concluded that the stiffness modulus at − 15 ℃ almost remains constant, while that at 15 ℃ presents a few enhancements as the velocity increases. It shows that the internal stress and strain of a linear elastic material have no correlation with the external loading velocity in theory. But the loading velocity has a certain influence on the EAM due to its viscoelastic and heterogeneous properties at 15 ℃. When the velocity increases from 1 to 50 mm/min, the stiffness modulus increases by 12. 3% at 15 ℃. In addition, the increment when the velocity increases from 1 to 30 mm/min is more than that from 30 to 50 mm/min.

The EAM has the characteristic of stress relaxation since the viscoelasticity, namely the stress, will reduce to some extent under constant strain loading. When the loading velocity is slow, the internal material presents energy consumption and the modulus declines.

Actually, the asphalt binder makes the mixture viscoelastic (Aggregates are considered linear elastic). Therefore, the influences of loading velocity are related to the character of aggregates, the amounts of asphalt binder, the distribution of mastic and the loading path, etc.

The interior point of aggregate A, the contact point I_A, I_M between the aggregates and the asphalt mastic, and the internal point of mastic M are selected to study the distribution of localized stress, as shown in Fig. 8. Because the loading velocity has no effect on the model at − 15 ℃, the model characterized by viscoelastic properties at 15 ℃ is studied. Under controlled-strain loading (the deflection of sample is 0. 5 mm), the localized stress is computed and shown in Tab. 4.
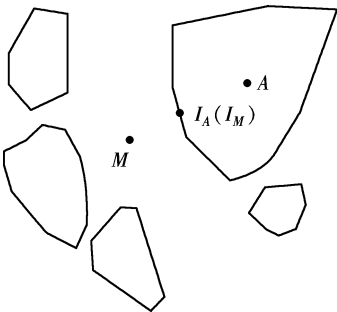

Fig. 8   Analysis points in local zone

Tab. 4   Influence of loading velocity for stress in local zone

Loading velocity/ (mm · min^{-1})	Stress(15 ℃)/MPa			
	A	I_A	I_M	M
1	3. 51	1. 04	1. 01	0. 67
10	3. 69	1. 11	1. 09	0. 73
30	4. 0	1. 2	1. 19	0. 79
50	4. 21	1. 25	1. 25	0. 82

It can be noticed that the loading velocity has a certain influence on the localized stress of the mixture's interior. When the velocity increases from 1 to 50 mm/min, the stresses of A, I_A, I_M and M increase by 19. 9%, 20%, 23. 7% and 22. 4%, respectively. Furthermore, the stresses

Fig. 7   Influence of loading velocity on stiffness modulus.
(a) − 15 ℃; (b) 15 ℃

at the aggregate point, the contact point and the mastic point present an attenuation trend, which indicates that aggregates with high moduli sustain stronger stress than that of the mastic with low moduli. Meanwhile, the stress distribution of the contact between the aggregate and the mastic is completely continuous as the stress value of I_A and I_M is almost the same.

The stress relaxation of the mixture requires some time for the stress to reduce to some extent. When the loading velocity increases, the sample breaks but there is no time for the internal stress to relax. Therefore, the stress under controlled-strain loading will increase as the loading velocity increases. In addition, the influences of the stress increase are related to the gradation, viscoelasticity of asphalt binder, and the distribution of the microstructure in loading path, etc.

3 Conclusions

1) The stress distribution of the internal microstructure indicates that aggregates with high moduli sustain higher stress than that of the mastic with low moduli, while the strain distribution indicates the opposite.

2) Model simulation results of the stiffness modulus in IDT match well with those obtained from laboratory tests, which suggests sound material parameters and the validity of the finite-element numerical simulation results.

3) The loading direction has some influence on the splitting stiffness modulus, and the moduli of different loading directions are different. Meanwhile, the stiffness modulus in each direction presents some statistical characteristics, and there is little diversity among the moduli of vertical, horizontal and inclined at 45° to the left. Therefore, it is suitable to use parallel tests with several samples in order to obtain greater test effects.

4) Because the mastic at −15 ℃ is defined as linear elastic, the loading velocity has no effect on the stiffness modulus. However, the modulus at 15 ℃ presents a few enhancements when the loading velocity increases due to the stress relaxation of the mastic. In addition, the localized stresses at 15 ℃ in different microstructure zones increase as the loading velocity increases.

References

[1] You Z, Dai Q. Dynamic complex modulus predictions of hot-mix asphalt using a micromechanical-based finite element model [J]. *Canadian Journal of Civil Engineering*, 2007, **34**(12): 1519−1528.

[2] Bahia H U, Zhai H, Bonnetti K, et al. Non-linear viscoelastic and fatigue properties of asphalt binders [J]. *Journal of the Association of Asphalt Paving Technologists*, 1999, **68**:1−34.

[3] Kose S, Guler M, Bahia H U, et al. Distribution of strains within hot-mix asphalt binders [J]. *Transportation Research Record*, 2000,**1391**:21−27.

[4] Yu J M, Li X J, Wang D Y, et al. Finite element modeling of asphalt mix with x-ray computerized tomography processing [J]. *Journal of Chang'an University*: *Natural Science Edition*, 2006, **26**(1): 16−19. (in Chinese)

[5] Abbas A R, Papagiannakis A T, Masad E A. Linear and nonlinear viscoelastic analysis of the microstructure of asphalt concretes [J]. *Journal of Materials in Civil Engineering*, 2004, **16**(2): 133−139.

[6] Papagiannakis A T, Abbas A R, Masad E A. Micromechanical analysis of viscoelastic properties of asphalt concretes [J]. *Transportation Research Record*, 2002, **1789**: 113−120.

[7] Luo S, Wang J W, Qian Z D. Research on the performance of locally developed epoxy asphalt mixture [C]//*Proceedings of the 26th Annual Southern African Transport Conference*. Pretoria, South Africa, 2007: 736−744.

[8] Abbas A. Simulation of micromechanical behavior of asphalt mixtures using discrete-element method [D]. Pullman, WA, USA: Department of Civil and Environmental Engineering of Washington State University, 2004.

[9] Huang W. *Theory and method of deck paving design for long-span bridges*[M]. Beijing: China Construction Industry Press, 2006. (in Chinese)

[10] Wang H N. Research on numerical simulation of the asphalt mixture microstructure [D]. Xi'an: Highway School of Chang'an University, 2007. (in Chinese)

[11] Ministry of Communications. JTJ 052—2000 Standard test methods of bitumen and bituminous mixtures for highway engineering [S]. Beijing: China Communications Press, 2000. (in Chinese)

[12] Dai G. Research on the performance of diabase used in the epoxy asphalt mixture [D]. Nanjing: School of Transportation of Southeast University, 2010. (in Chinese)

基于细观结构有限元模型的环氧沥青混合料间接拉伸试验研究

王江洋　　　钱振东

(东南大学智能运输系统研究中心,南京 210096)

摘要:运用有限元方法建立环氧沥青混合料细观结构模型,对其间接拉伸试验(IDT)进行数值模拟.首先借助图像处理技术得到由集料和沥青砂浆组成的环氧沥青混合料二相细观结构,并通过蠕变试验获取沥青砂浆常温下的黏弹性材料参数,最后结合有限元手段建立包含集料、砂浆等在内的混合料细观结构有限元模型.数值模拟结果表明,有限元计算的混合料劲度模量与实际 IDT 试验结果吻合较好,通过改变加载方向、加载速率等参数,发现对混合料细观结构的劲度模量以及局部点位应力均造成一定影响,分析主要原因可能是由沥青混合料的内部结构分布不均匀性以及沥青砂浆的黏弹性特点所造成.研究成果可为微观有限元方法进一步推广应用于不同条件下沥青混合料微观力学响应仿真提供理论依据.

关键词:微观结构;环氧沥青混合料;图像处理技术;有限元模型;间接拉伸试验

中图分类号:U443.33